ALKALINE ELECTROLYSIS CFD MODELING AND APPLICATION: A NOVEL EXPRESSION FOR A VOLUME FRACTION-DEPENDENT CURRENT DENSITY

Marco Dreoni[1], Francesco Balduzzi[1]*, Francesco Maria Ferro[2], Matthias Neben[3], Syed Sahil Hossain[3], Giovanni Ferrara[1], Alessandro Bianchini[1]

[1] Department of Industrial Engineering, Università degli Studi di Firenze, Via di Santa Marta 3, 50139, Firenze, Italy

[2] McPhy Energy Italia Srl, Via Ayrton Senna 22, 56028, San Miniato, Italy

[3] McPhy Energy Deutschland GmbH, Schwartzkopffstraße 1, 15745, Wildau, Germany

*Corresponding Author: francesco.balduzzi@unifi.it

ABSTRACT

To enhance the design and efficiency of alkaline water electrolyzer cells, the use of Computational Fluid Dynamics (CFD) is imperative, particularly through multiphysics simulations, able to account for electrochemical phenomena and multiphase flows. Despite noteworthy studies in the literature, the validation of CFD results through detailed experimental measurements remains to date limited and the modeling approach uncertain. Furthermore, most of the studies do not consider the effect that gas accumulation on the electrodes has on the cell performance.
The first aim of the study is to evaluate the impact of some of the modeling choices for the CFD simulation of the electrochemical cell. In this context, a novel method concerning the use of an electrochemical module is employed. The two-phase model is validated against PIV experimental measurements for a literature case study of a zero-flux electrochemical cell. The results of the validation highlight a major resemblance to the experiments when a mass source term is employed. The use of electrochemistry is however crucial to ensure a more physical accuracy.
The second phase of the study involves the application of the developed model on a 2.5D sector of a real-scale cell of a 1 MW electrolyzer to assess the velocity and volume fraction behaviors at the cathode for various current density values, ranging from 1,000 to 10,000 A/m². Sensitivity analyses are conducted to identify which is the impact of different electrolyte mass flow rates and current densities on the cell. Special attention is dedicated to the impact of gas accumulation on the electrode, by introducing a new function for the current density, with dependence on the local volume fraction. In particular, the ratio between the average electrode and outlet gas volume fraction is considered as a key performance indicator, to evaluate the effect of bubble coverage. The main output observed is that gas accumulation is enhanced by lower current densities and higher mass flow rates.

1 INTRODUCTION

Electrolysis-based hydrogen production represents a viable solution to address the challenge of electricity storage arising from the growing utilization of renewable energy sources. Among the common water electrolysis systems, alkaline water electrolyzers (AWEs) are characterized by a lower installation cost range, around 500 / 1,000 USD/kW (Wang *et al.*, 2023), and this makes them suitable for large-scale green hydrogen projects. Furthermore, AWE systems efficiently absorb fluctuating energy outputs from renewables, when operated dynamically (Zhang *et al.*, 2021).
Finding a way to accurately simulate the effect of gas accumulation and bubble coverage inside AWE cells is crucial for enhancing its electrochemical performance and overall efficiency. According to Zeng and Zhang (2010) bubble resistance is the main contribution to the total energy loss in AWEs. Furthermore, bubbles have a double effect: the ones attached to the electrode contribute to reducing the

https://doi.org/10.52202/077185-0073

effective area for the reaction, whereas the ones detached from electrode increase electrolyte resistivity (Hine and Murakami, 1980). Aldas *et al.* (2008) thoroughly reviewed the literature concerning the influence of the main physical parameters on the bubble coverage of an electrode, showing how electrolyte velocities and current densities impact the gas volume fraction.
Optical techniques often fail due to high gas fraction, making Computational Fluid Dynamics (CFD) essential. However, consensus on suitable CFD models and methods for simulating cell hydrodynamics is lacking, given limited validation against experimental data. A review of the relevant literature on the subject will be shown in the next chapter.
In continuation with the previous work by the authors (Dreoni *et al*., 2022), this paper builds upon the findings and methodologies presented to further investigate the CFD modeling of alkaline electrolyzers and to expand the research by assessing the influence of a new gas introduction approach, i.e. through electrochemical reactions at the electrodes. To the best of the author's knowledge, the use of electrochemistry for gas introduction in Fluent® software has not been documented for an alkaline electrolyzer cell. Due to the possibility of directly linking the current density to the local volume fraction, this method presents a potential avenue for more physically accurate simulations.
The final step of the current research involves the use of the studied model on a simplified cell geometry of an alkaline electrolyzer produced by McPhy, to assess its impact on gas accumulation inside the cell and allow the evaluation of the main variables involved.
Performing fluid-dynamics optimization allows for the reduction of gas residence time at the electrode. According to Angulo *et al*. (2020), bubbles removal through ultrasonic field leads to a possible decrease of the cell potential by 10-25%, thereby increasing the faradaic efficiency. These percentages give an idea of the impact of the gas accumulation inside the cell on its performance.
The paper is organized into five sections. It begins with a brief review of CFD models commonly employed in the literature for gas introduction inside the electrochemical cells and includes a new gas generation approach by means of a novel current density function. Chapter 3 provides an overview of both the literature case study for validation and the details concerning the employed real cell. Chapter 4 details the numerical model setup, covering aspects such as geometry, mesh construction and the specific models and forces utilized within the Fluent® software. Finally, Chapter 5 and Chapter 6 present the obtained results and conclusions based on the findings.

2 MODELING APPROACHES FOR GAS GENERATION

In two-phase liquid-gas flows, two primary fluid-dynamics models are commonly employed: Euler-Euler and Euler-Lagrange. The former describes both phases using transport equations on a fixed coordinate system, while the latter treats the electrolyte solution as a continuous phase and the bubbles as discrete particles. Within the present analysis a Euler-Euler model was employed and special attention was given to the modeling of gas introduction inside the cell.

2.1 Gas introduction as source terms or wall fluxes

In existing literature, CFD models commonly rely on source terms or mass-flow inlet techniques to introduce hydrogen and oxygen gas into electrochemical cells. Several studies have adopted these approaches. A mass source term was employed by Xue *et al.* (2024), by Le Bideau *et al.* (2020), who considered the first layer of cells adjacent to the electrode wall for introducing the gas, and by Zarghami *et al.*(2020), whose layer of gas generation was taken as thick as the bubble diameter.
Faraday's law is generally employed to calculate the mass source term:

$$M = i \cdot A / (F \cdot z), \tag{1}$$

where M represents the mole flow (mol/s) of hydrogen, or oxygen, i is the current density (A/m^2), A is the electrode surface (m^2), F=96,487 (A·s/mol) is the Faraday constant and z is the number of electrons involved in the electrochemical reactions, equal to 2 for hydrogen evolution reaction at cathode and 4 for oxygen evolution reaction at anode. The two electrochemical reactions for alkaline water electrolysis are displayed below:

https://doi.org/10.52202/077185-0073

Cathode: $$2H_2O_{(l)} + 2e^- \rightarrow H_{2(g)} + 2OH^-_{(aq)} \quad (2)$$

Anode: $$2OH^-_{(aq)} \rightarrow \frac{1}{2}O_{2(g)} + H_2O_{(l)} + 2e^- \quad (3)$$

On the other hand, Mat *et al.*(2004) and Aldas *et al.* (2008) applied a boundary condition as mass-flow inlet for the gas generation, using Faraday's law to calculate the normal velocity of gas at electrodes. Finally, Rodríguez and Amores (2020) employed a segregated approach, with imposition of current density to reproduce the electrochemical behavior and a mass flux at electrodes for the fluid-dynamics modeling. The main limitation of such approaches is the inherent uniformity of the gas generated that cannot consider the local bubble coverage effect, i.e. the gas curtain on the electrode constituting an electrical resistance for the cell.

2.2 Gas generation by means of electrochemistry

The use of an electrochemical module allows for the introduction of the gas through electrolysis reactions. The amount of gas is calculated based on the current density defined as boundary condition at the electrode.

Compared to other ways of introducing the gas, its main advantage consists in enabling the analysis of different electrical parameters and variables, e.g. the potential field inside the cell. Plus, it is more easily possible to establish a dependence of the local current density on the gas volume fraction and to consider their mutual influence, as shown in Equations (4) and (5).

The common equation employed for the electrode current density is the one employed by Mat *et al.*(2004) and Aldas *et al.* (2008):

$$i = i_o \cdot (1 - VF) \cdot \exp(-F\eta/2RT), \quad (4)$$

where i_o is the exchange current density (A/m^2), VF the volume fraction (-), F is the Faraday constant, η the overpotential (V), R the ideal gas constant (J/mol K) and T the temperature in K.

A novel function for the current density is here presented. As shown in Equation (5) below, the electrical quantity is directly dependent on the local volume fraction, with the aim of replicating the phenomenon of bubble coverage:

$$i_{var} = i_{ave} \cdot (1 - VF)/(1 - VF_{ave}), \quad (5)$$

where i_{var} is the variable current density (A/m^2), defined cell by cell, i_{ave} the average electrode current density (A/m^2), VF the local volume fraction for the gas phase (-), and VF_{ave} the average electrode volume fraction (-), calculated for each iteration. A reduced local current density is expected where the gas is more highly present, hence i_{var} decreases with the height of the cell, while having a constant average current density, dependent on the current applied.

The new approach proposed by the authors is a trade-off between the imposition of a constant current density at the electrode, and Equation (4). This electrochemical method for gas generation is useful when the potential field cannot be solved for any reason (e.g. the lack of data).

3 EMPLOYED CASE STUDY AND ELECTROLYZER CELL

3.1 Case study

The present study analyzes a test case taken from Hreiz *et al.* (2015) and employed by the authors for a previous work (Dreoni *et al.*, 2022) as shown in Figure 1.

This particular zero-flux reactor is part of a larger setup including both anodes and cathodes. However, the object of the study is only the region between the anodes, thus only oxygen is produced inside the domain. The choice of such a reactor over a traditional electrolysis cell was based on its exceptional visualization of bubbles, making it an ideal case for analysis. In the paper by Hreiz *et al.* (2015), a PIV algorithm was employed to calculate the mean velocity field of the gas, which served as a benchmark for validating the numerical model. By utilizing the PIV-method results as a reference, the accuracy of

https://doi.org/10.52202/077185-0073

the numerical simulations could be assessed, providing valuable insights into the behavior of the gas phase in the studied system.

3.2 Electrolyzer Cell

A real-scale cell of a 1MW electrolyzer was employed for the application of the model. In particular, the reference case is the McLyzer 200-30, whose stack works at 30 bar of pressure with a production of 200 Nm³/h of hydrogen. The analysis involved the simulation of the cathodic half-cell, i.e. the portion of electrolyzer cell which lies between the cathode and the bipolar plate. Hence, only the hydrogen evolution at the cathode is modeled. The geometry details of the cell cannot be disclosed since they are proprietary information of the company. A 2.5D vertical sector of the circular cell is analyzed in the present paper, as highlighted in the schematic of Figure 2.

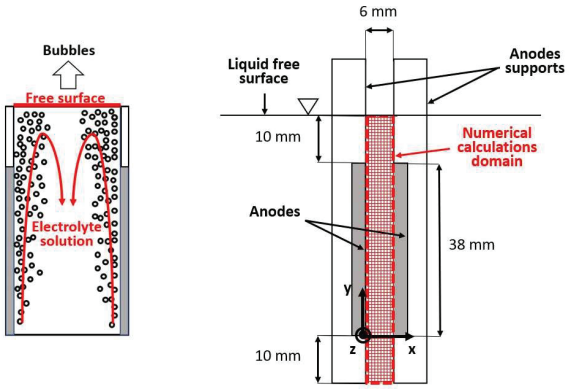

Figure 1. No Net Flow Configuration (NNFC) of the electrochemical reactor and cell geometry

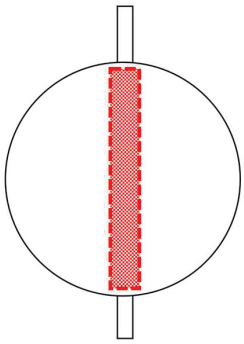

Figure 2. Schematic of the AWE cell domain

4 NUMERICAL MODEL SETUP

4.1 Test-case cell

The numerical modeling of the cell was conducted within ANSYS® 2023 R1 software program and the fluid-dynamics simulations were performed in Fluent®.

4.1.1 Computational domain: The geometry was created using Design Modeler® and aligned with the specific study-case domain. To enhance stability, the bottom part of the domain was extended 10 mm below the anode segments.

The mesh resolution was selected according to the limitation imposed by the two-phase model. Indeed, based on the diameter of the gas bubble generated, the minimum size of the mesh cells should be able to capture the size of the gas bubbles. Picardi *et al*. (2020) had established an optimum ratio of $1/\sqrt{2}$

https://doi.org/10.52202/077185-0073

between bubble diameter and grid size. In the present case, an element size of 0.15 mm and 0.125 mm in the direction of cell thickness were chosen to accurately capture the small bubble size (0.1 mm). The final mesh consisted of approximately 500,000 elements.
However, to evaluate the numerical error related to the spatial resolution, a grid sensitivity analysis was performed by progressively increasing the elements size (X [mm], Y [mm], Z [mm]), showing a grid-independent behavior.

4.1.2 Fluid-dynamic model: Due to the dispersed state of bubbles, the two-phase Eulerian model was employed, with the following hypotheses:

- The pressure is uniform and equal to atmospheric pressure for both phases.
- The flow is Newtonian, incompressible and viscous.
- The cell is assumed to be isothermal, with temperature T=20 °C, according to the experimental setup (Hreiz *et al.*, 2015).
- The flow is laminar due to the low flow velocities and the pressure gradients are negligible.
- The current density distribution is taken as uniform.
- The bubbles dimension is considered constant and spherical, equal to 0.1 mm.
- Bubble coalescence and breakage are neglected.

The primary force governing the movement of bubbles within the cell is the buoyancy force, arising from the substantial density difference between the electrolyte and oxygen, which are 1,020 kg/m³ and 1.30 kg/m³, respectively. The Ishii-Zuber model was employed for the drag force, as indicated by Khan *et al.* (2020). A surface tension of 72 mN/m, equal to the one of water at room temperature, was considered. Finally, two other forces were activated in the model, i.e. a wall lubrication force, expressed with Antal *et al.* equation, and a virtual mass force, with a 0.5 coefficient, consistent with the spherical hypothesis for the bubbles.
A stationary no-slip wall was assigned to the anodes, and a degassing condition was used as outlet boundary.

4.1.3 Gas introduction approaches: Three different approaches for the gas introduction were tested for the validation case. First, a mass source term was adopted, by considering a thin layer of 0.4 mm at the electrode. The second approach involved using mass-flow inlets at electrodes. Due to the low amount of gas produced, the impact of mass fluxes on the velocity field is low in the direction normal to the electrode, hence such approach is justified. For the third case, electrochemical reactions at the electrodes were employed. A constant current density was in this case applied, equal to 130 A/m², being the volume fraction low and thus not relevant to use Equation (5).

4.2 Electrochemical model application to simplified half-cell of real-case electrolyzer

As already mentioned, the developed Fluent® model was applied to the simplified geometry of an alkaline electrolyzer cell, with the fluid-dynamic model differences described in Paragraph 4.2.2.

4.2.1 Computational domain: A hexahedral mesh was built with a strong refinement at the cathode and a grid independence test was performed. Since in this case the diameter of gas bubbles was considered to be 10 µm, a finer mesh could be conducted and, in particular, different cases were analyzed, from 20-µm to 200-µm minimum size at the electrode. The 50 and 100-µm cases behaved almost identically in terms of volume fraction and velocity. Thus, the second one was considered, for the lower computational costs related. What could be observed instead was an important flow instability for the 20-µm case. A calculation of the volume of gas could in fact determine that a minimum size of 40 µm had to be used, not to have a volume of cell lower than the local amount of gas produced at the electrode. It is therefore necessary to do a trade-off between the gas bubble size and the gas production, to find the minimum layer thickness at the electrode for stable simulations:

$$L_{min} = MAX(d_b\,; V_g/A), \tag{6}$$

https://doi.org/10.52202/077185-0073

where d_b is the bubble diameter (m), V_g is the volume of the gas generated in the first layer of cells at the electrode (m^3) and A is the electrode surface (m^2).

4.2.2 Fluid-dynamic model: The assumptions for Fluent® model were the same of the validation case, with the following differences:

- Inlet temperature and operating pressure were chosen equal to 60 °C and 30 bar, consistently with the real application.
- Primary phase is a 28 wt% solution of KOH in water, whereas secondary phase is hydrogen.
- The flow regime was set as turbulent, employing a k-ω SST model with low Reynolds correction. In fact, velocities are in this case higher than the no net flow cell, being the electrolyte recirculated.
- The bubble diameter for hydrogen gas was chosen to be 10 µm, i.e. ten times smaller than the test case, due to the higher pressure and the different secondary phase (hydrogen instead of oxygen).
- The surface tension was chosen to be 60 mN/m, i.e. about the one of water at the selected pressure and temperature.

Regarding the boundary conditions, a pressure-outlet condition was used at the outlet and a mass flow at the inlet, calibrated to give the same gas volume fraction as the real cell at the outlet. Both constant and variable current densities, by means of Equation (5), were employed for the analysis.

5 RESULTS

5.1 Test-case cell results

The main parameter considered, to evaluate the accuracy of the models described, was the gas vertical velocity in the mid-section. This output was compared to the bubbles velocity fields that Hreiz *et al.*(2015) were able to obtain. The three different cases of gas introduction were compared to the experimental results at 130 A/m^2, as shown in Figure 3.
Among the three approaches, the one using the mass-flow inlet at the electrodes gave the highest maximum velocities, compared to the experiments, whose maximum is around 0.02 m/s. The introduction of gas through source term provided a maximum value that is more similar to the experimental output, while the velocity reached by the electrochemical module application was slightly lower. Notwithstanding the minor correspondence of the electrochemical approach to the measurements, its use is more physically significant and it allows to access other multiphysics variables, otherwise absent, such as the potential field inside the cell. Furthermore, it is important to point out that larger bubbles were not included in the model, whereas up to 1 mm-size bubbles appear to be created close to the electrode increasing local turbulence and velocity diffusion, as it is evident from the pictures and videos taken by Hreiz *et al.* (2015).

5.2 Electrolyzer cell results

The application of the CFD model with the electrochemical approach on the 2.5D sector of a real-scale cell of a 1 MW electrolyzer allowed to conduct a sensitivity analysis on the main variables involved. First, the novel equation for current density, as written in Equation (5) was compared to a constant current density case (at 10,000 A/m^2) and employed for three different cases, i.e. i_{ave} of 1,000, 5,000 and 10,000 A/m^2, to evaluate the output in terms of gas vertical velocity and volume fraction. Secondly, the 5,000 A/m^2-case was employed to assess the impact of a variable electrolyte flux at the inlet, by considering half and double mass flow cases, with respect to the nominal one.

5.2.1 Impact of constant and variable current densities: By using Equation (5), the electrode current density is not uniform, but its value decreases with increasing height as shown in the graphs of Figure 4 for the 10,000 A/m^2-case. The impact of the new expression of current density was evaluated with respect to the constant current density. Being a no-slip condition applied at the wall, a line close to the electrode was considered, at a distance of 100 µm, for the velocity graph.

https://doi.org/10.52202/077185-0073

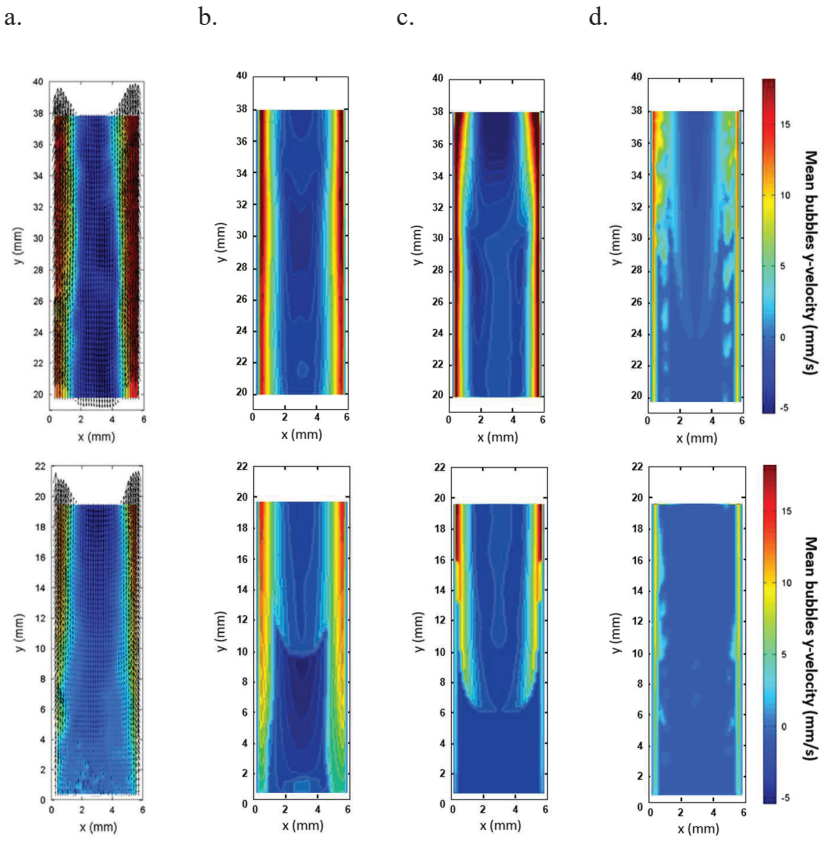

Figure 3. Mean gas y-velocity contour plots of test-case cell for i=130 A/m^2. (a) PIV output from experimental results (Hreiz *et al.*, 2015). (b) Introduction of gas by means of source term, (c) mass-flow inlets and (d) electrochemical module.

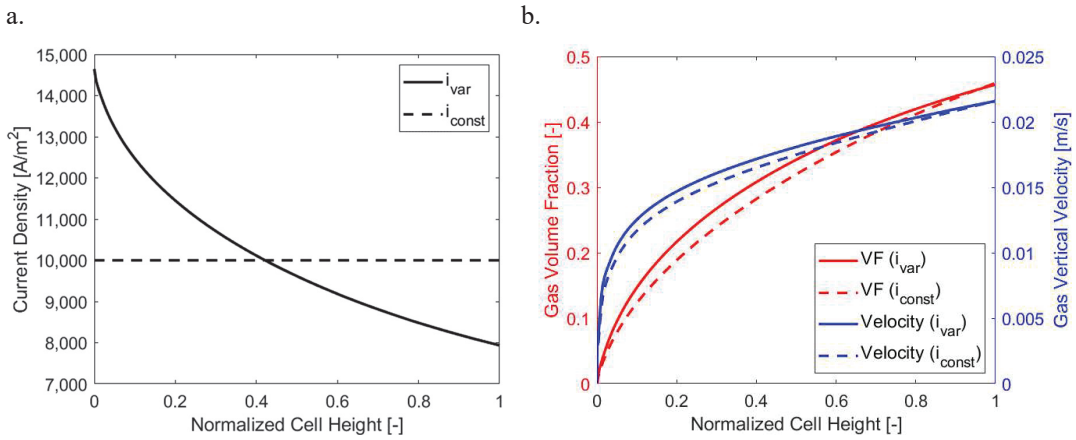

Figure 4. (a) Electrode current density and gas volume fraction as a function of AWE cell height for i_{ave}=10,000 A/ m². (b) Impact of constant and variable current density on gas vertical velocity and volume fraction as a function of cell height for i_{ave}=10,000 A/m².

https://doi.org/10.52202/077185-0073

The impact of the variable current density, compared to the constant one, was noticeable on the gas vertical velocity and volume fraction at the electrode, especially in the first quarter of the cell height, where the gas velocity and volume fraction were, on average, respectively around 10 % and 20 % higher than the constant current density case. As expected, we see an increased hydrogen production in the low part of the cell, where the bubble coverage is lower and, thus, absorbed current density higher, with consequent larger values of gas volume fraction and vertical velocity.
Thus, it is confirmed that the approach of having a variable current density is numerically more consistent than the constant one, where no mutual influence of the gas volume fraction on the local current density is considered.

5.2.2 Sensitivity analysis on variable current density: By varying the average current density, the graph reported in Figure 5 was obtained, in terms of current density and gas volume fraction. The quantities were normalized by the average electrode gas volume fraction and electrode current density, to better highlight the relative variation of the trend when reducing hydrogen production. It is clear from the chart that the variable current density function is more significant when the average current density is higher.
In Table 1 are reported the values of outlet and electrode average gas volume fraction for the three cases studied. The ratio between them can be considered as a key performance indicator for the cell, when conducting a design based on CFD simulations. A value higher than 1 means a larger amount of gas accumulation since, in such cases, the average gas volume fraction at the outlet is lower than the average one at the electrode.

Table 1: outlet and electrode average gas volume fraction values and their ratio

i_{ave} [A/m²]	VF_{ave} [-]	VF_{out} [-]	VF_{ave}/VF_{out} [-]
1,000	0.08	0.05	1.60
5,000	0.21	0.22	0.95
10,000	0.32	0.37	0.86

Also, the trends of gas vertical velocity and volume fraction for the three values of average current density are reported in the charts of Figure 6. The gas velocity decreases away from the electrode, whereas the volume fraction remains constant after a first abrupt decline. The peaks of velocity correspond to the buoyancy effect given by the gas production.

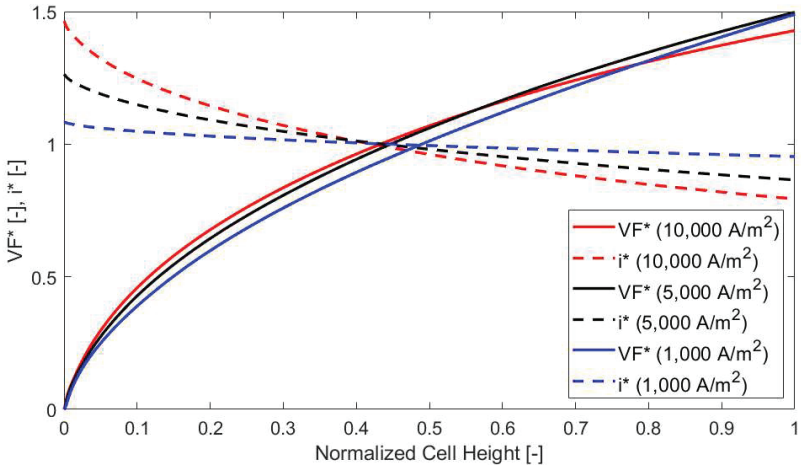

Figure 5. Normalized values of current density (i*) and volume fraction (VF*) for i_{ave}=1,000/5,000/10,000 A/m², as a function of cell height.

https://doi.org/10.52202/077185-0073

5.2.3 Sensitivity analysis on electrolyte mass flow rate: Two additional values of electrolyte mass flow rates were evaluated, corresponding to half and double amounts of the nominal flux (m). The gas vertical velocity and volume fraction trends for i_{ave}=5,000 A/m² are reported in the graphs of Figure 7. An increase in mass flow rate determines a raise in the flow velocity. In turn, the volume fraction shows a decrease. As already mentioned, gas accumulation at electrode is to be avoided, being the gas bubbles a source of electrical resistance.

5.2.4 Discussion: The outlet average gas volume fraction trend for the different electrolyte flow rates and current densities is reported in the chart of Figure 8a. In Figure 8b the trend of the ratio between outlet and electrode average gas volume fraction is instead displayed.
Such analysis shows that when the mass flow rate is doubled the average volume fraction at the outlet is on average around 40 % lower and, when it is halved, 60 % higher. Therefore, the impact of the mass flow rate is significant on the cell performance, also considering that the overall hydrogen production is the same for each i_{ave} considered. On the other hand, the ratio VF_{ave}/VF_{out} is higher for higher values of mass flow rate, meaning a relative more significant gas accumulation at the electrode. In fact, as VF_{out} increases, it can be observed that the ratio tends to decrease. This implies that the more hydrogen is produced, the more diffusion towards the center of the cell occurs, whereas, when hydrogen production is low, the gas remains closer to the electrode, without diffusing inside the cell. On the other hand, higher current densities mean a higher possibility for the gas to spread inside the cell, mixing with the electrolyte that is far from the electrode.

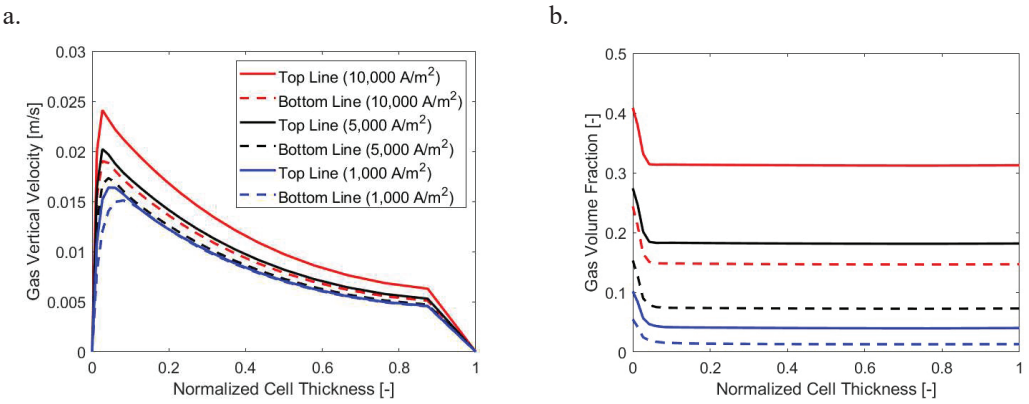

Figure 6. Gas vertical velocity (a) and gas volume fraction (b) along the thickness of the cell for i_{ave}=1,000/5,000/10,000 A/m², at a quarter and three quarters of cell height.

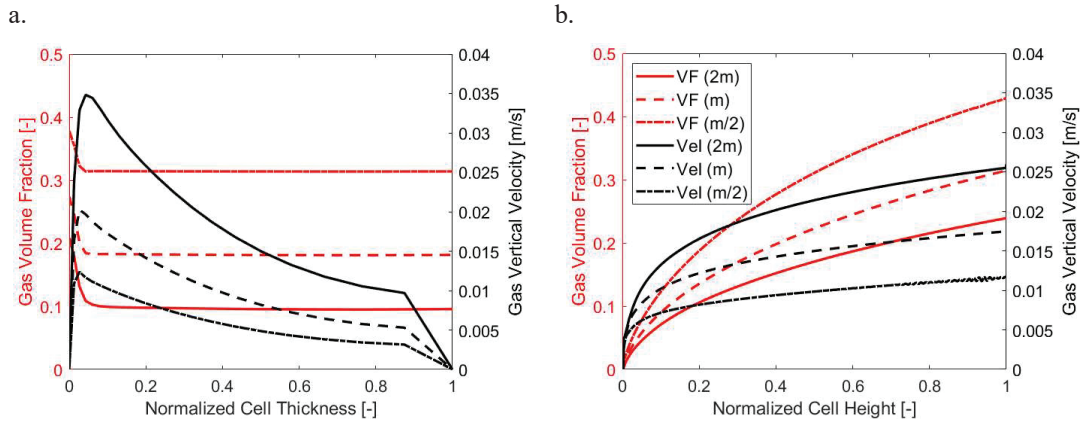

Figure 7. Gas vertical velocity and volume fraction along the thickness at three quarters of cell height (a) and along the height of the cell (b) for the three mass flow rates, for i_{ave}=5,000 A/m².

https://doi.org/10.52202/077185-0073

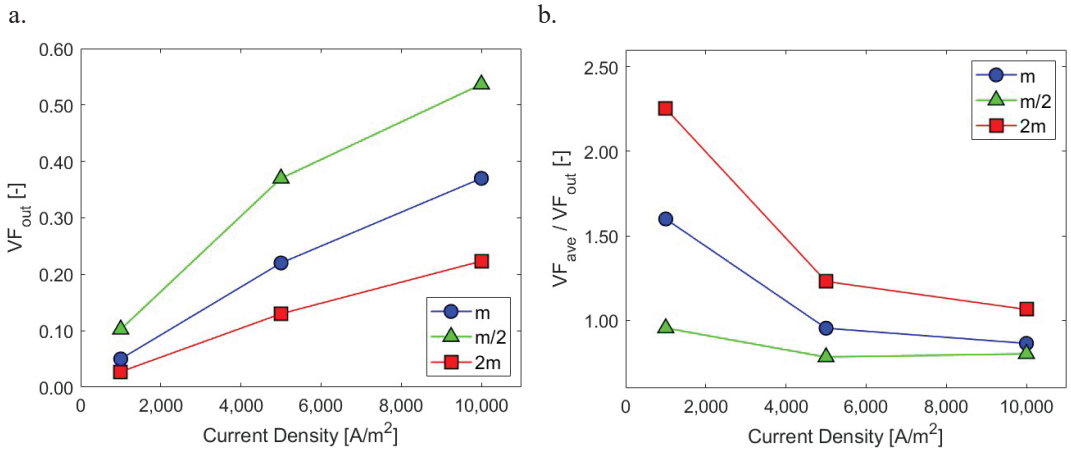

Figure 8: (a) Outlet average gas *VF* values and (b) ratio VF_{ave}/VF_{out} for the cases studied.

6 CONCLUSIONS

To date, few validated CFD studies on alkaline water electrolysis are available. Different approaches to simulate what happens in an AWE cell are shown by the literature, with little agreement. The first aim of the paper was to present a comparison of some of these approaches, introducing a novel method, i.e. the use of an electrochemical module in Fluent® software, by validating it against a literature study-case. The second goal was to present the output when electrochemistry is applied on a 2.5D sector of a real-scale electrolyzer cell, with a new current density definition at the electrode, to consider the effects of bubble coverage.

The best fit by comparison to the experimental results from literature was obtained for the case of gas introduction through source term. Use of gas fluxes at the electrodes determined instead higher vertical velocities, while the use of the electrochemical module had a lower resemblance to measurements. However, the physical significance of the last approach was considered noteworthy, together with the possibility of evaluating electrical parameters, otherwise absent.

Concerning the model application to the real-case cell, possible changes in operational parameters, such as the average current density and electrolyte mass flow, were evaluated and the ratio between electrode and outlet average gas volume fraction, VF_{ave}/VF_{out}, was employed as key performance indicator. It could be observed that higher current densities mean a relative lower gas accumulation at the electrode surface, since the gas tends to spread towards the centre of the cell. Doubling or halving the electrolyte flow rate has a noticeable impact on the gas volume fraction. For instance, a sensitivity analysis showed that a double mass-flow rate at the inlet determines a reduction of about 40 % for the average outlet volume fraction, that is in turn raised by 60 % when the mass flow rate is halved. Conversely, when the mass flow rate is increased, there is a higher VF_{ave}/VF_{out} ratio, indicating a relatively more substantial accumulation of gas at the electrode.

Future developments of the model include the refinement of the electrical modeling. In fact, to have a sound characterization of the current density, precise and case-related values of Tafel or Butler-Volmer equations are to be known, such as Tafel slopes for cathode and anode, Butler-Volmer coefficients or exchange current densities.

Finally, from the fluid-dynamics point of view, the inclusion of the so-called very large bubbles, might be crucial to better match the real flow field, e.g. through the use of a population balance model.

NOMENCLATURE

A	electrode surface	(m^2)
AWE	alkaline water electrolyzer	
CFD	computational fluid dynamics	

https://doi.org/10.52202/077185-0073

d_b	gas bubble diameter	(m)
η	overpotential	(V)
F	Faraday constant	(A s/mol)
i	current density	(A/m^2)
i_0	exchange current density	(A/m^2)
L_{min}	minimum thickness of layer	(m)
m	nominal mass flow rate	(kg/s)
M	mole flow	(mol/s)
MAX	maximum value	
NNFC	no net flow configuration	
PIV	particle image velocimetry	
R	ideal gas constant	(J/mol K)
T	temperature	(K)
USD	United States dollar	
V_{gas}	volume of gas	(m^3)
VF	volume fraction	(-)
X,Y,Z	axis directions	
z	number of electrons	(-)

Subscript

aq	aqueous
ave	average
g	gas
l	liquid
out	outlet
*	dimensionless

REFERENCES

Aldas, K., Pehlivanoglu, N., Mat, M.D., 2008, Numerical and experimental investigation of two-phase flow in an electrochemical cell, *International Journal of Hydrogen Energy*, TMS07: Symposium on Materials in Clean Power Systems, vol. 33: p. 3668-3675.

Angulo, A., Van der Linde, P., Gardeniers, H., Modestino, M., Rivas, D. F., 2020, Influence of bubbles on the energy conversion efficiency of electrochemical reactors, Joule, vol. 4.3: p. 555-579.

Dreoni, M., Balduzzi, F., Ferrara, G., Bianchini, A., 2022, Accuracy Assessment of the Eulerian Two-phase Model for the CFD Simulation of Gas Bubbles Dynamics in Alkaline Electrolyzers, J. Phys.: Conf. Ser, vol. 2385: p. 012040.

Hine, F., Murakami, K., 1980, Bubble Effects on the Solution IR Drop in a Vertical Electrolyzer Under Free and Forced Convection, *J. Electrochem. Soc.*, vol. 127: p. 292.

Hreiz, R., Abdelouahed, L., Fünfschilling, D., Lapicque, F., 2015, Electrogenerated bubbles induced convection in narrow vertical cells: PIV measurements and Euler–Lagrange CFD simulation, *Chemical Engineering Science*, vol. 134: p. 138-152.

Khan, I., Wang, M., Zhang, Y., Tian, W., Su, G., Qiu, S., 2020, Two-phase bubbly flow simulation using CFD method: A review of models for interfacial forces, *Progress in Nuclear Energy*, vol. 125: p. 103360.

Le Bideau, D., Mandin, P., Benbouzid, M., Kim, M., Sellier, M., Ganci, F., Inguanta, R., 2020, Eulerian Two-Fluid Model of Alkaline Water Electrolysis for Hydrogen Production, *Energies*, vol. 13: p. 3394.

Mat, M.D., Aldas, K., Ilegbusi, O.J., 2004, A two-phase flow model for hydrogen evolution in an electrochemical cell, *International Journal of Hydrogen Energy*, *Fuel Cells*, vol. 29: p. 1015-1023.

Picardi, R., Zhao, L., Battaglia, F., 2016, On the Ideal Grid Resolution for Two-Dimensional Eulerian Modeling of Gas–Liquid Flows, *Journal of Fluids Engineering*, vol. 138.

Rodríguez, J., Amores, E., 2020, CFD Modeling and Experimental Validation of an Alkaline Water Electrolysis Cell for Hydrogen Production, *Processes*, vol. 8, p: 1634.

https://doi.org/10.52202/077185-0073

Wang, T., Wang, J., Wang, P., Wang, F., Liu, L., Guo, H., 2023, Non-uniform liquid flow distribution in an alkaline water electrolyzer with concave-convex bipolar plate (CCBP): A numerical study, *International Journal of Hydrogen Energy*, vol. 48: p. 12200-12214.

Xue, L., Song, S., Chen, W., Liu, B., Wang, X., 2024, Enhancing Efficiency in Alkaline Electrolysis Cells: Optimizing Flow Channels through Multiphase Computational Fluid Dynamics Modeling, *Energies*, vol. 17: p. 448.

Zarghami, A., Deen, N.G., Vreman, A.W., 2020, CFD modeling of multiphase flow in an alkaline water electrolyzer, *Chemical Engineering Science*, vol. 227: p. 115926.

Zeng, K., Zhang, D., 2010, Recent progress in alkaline water electrolysis for hydrogen production and applications, *Progress in Energy and Combustion Science*, vol. 36: p. 307-326.

Zhang, C., Wang, J., Ren, Z., Yu, Z., Wang, P., 2021, Wind-powered 250 kW electrolyzer for dynamic hydrogen production: A pilot study, *International Journal of Hydrogen Energy*, vol. 46: p. 34550-34564.

ACKNOWLEDGEMENTS

The research project was partially financed by the European Union in the context of "Next Generation EU". In particular, authors from the University of Florence would like to thank the Italian government, who financed the project through the "National Recovery and Resilience Plan" (PNRR), and authors from McPhy would like to acknowledge the French government for the financial support coming from the "Plan de Relance".

https://doi.org/10.52202/077185-0073